Exploring the genetic diversity and population structure of *Mobula birostris* in two key aggregation zones in the Eastern Tropical Pacific

**Karla E. Rojas López[1,2], Juan José Guadalupe[1], Milton Gordillo-Romero[1],
Andrea Montero-Oleas[1], Diana A. Pazmiño[3], Michel Guerrero[3,4],
Maria de Lourdes Torres[1,2,3,*]**

[1]Laboratorio de Biotecnología de Plantas (COCIBA), Universidad San Francisco de Quito (USFQ), Diego de Robles y Vía Interoceánica, 170901 Cumbayá, Ecuador

[2]Instituto Biosfera, Universidad San Francisco de Quito (USFQ), Diego de Robles y Vía Interoceánica, 170901 Cumbayá, Ecuador

[3]Galapagos Science Center, Universidad San Francisco de Quito and University of North Carolina at Chapel Hill, San Cristóbal 200101, Galápagos, Ecuador

[4]Fundación Megafauna Marina del Ecuador, Proyecto Mantas Ecuador, 170519 Quito, Ecuador

ABSTRACT: The giant manta ray *Mobula birostris* is the largest ray species in the world. Little is known about its genetic composition in key aggregation sites such as the Galapagos Islands and Isla de la Plata, near the province of Manabi in mainland Ecuador. This study aimed to determine the genetic diversity and population structure of *M. birostris* in these 2 locations to better understand its connectivity and distribution in Ecuadorian oceanic waters and to assist in its conservation and appropriate management. A total of 127 samples from mainland Ecuador (2013–2018) and 21 samples from Galapagos (2019) were collected and analyzed using 8 microsatellite loci. Results showed a moderately high level of genetic diversity for giant manta rays from both sites (mainland Ecuador $H_e = 0.72$; Galapagos $H_e = 0.66$). Population structure analyses suggests the presence of 2 different populations in the Galapagos and mainland Ecuador. The different genetic compositions found for each location could be associated with the displayed resident behavior, linked to the formation of upwelling systems caused by oceanic currents that bring nutrient-rich waters to both sites year-round. Our genetic connectivity analysis confirmed low gene flow between these 2 locations, further rejecting the hypothesis of a single panmictic population of *M. birostris* in Ecuador. Taken together, these results provide valuable information about the genetic composition and diversity of the giant manta ray, an Endangered species which has been scarcely studied in the Eastern Tropical Pacific.

KEY WORDS: Genetic variability · Population structure · Conservation · Residency patterns · Ecuador · *Mobula birostris*

1. INTRODUCTION

The Mobulidae family comprises all manta and devil rays distributed globally throughout tropical and temperate oceanic waters (Couturier et al. 2015). Mobulids are large pelagic filter-feeding rays whose diet is mainly composed of planktonic animals (Burgess 2017, Bray 2018). These species are characterized by low reproduction rates (one pup every 1–3 yr) as well as long maturation times (3–6 yr for *Mobula alfredi*, 10 yr for *M. mobular*, unknown for *M. birostris*) (Dulvy et al. 2014, Stewart et al. 2018), characteristics

that lead to slow recovery rates and increased vulnerability for the group (Marshall et al. 2011a,b, O'Malley et al. 2013). The main threats for mobulids include targeted and bycatch fishing as well as habitat degradation and climate change (Couturier et al. 2012).

The giant manta ray *M. birostris* is the largest mobulid species, with individuals that measure up to 7 m in disc width and weigh up to 2 t (Marshall et al. 2009, McClain et al. 2015). This species shows a preference for pelagic, offshore habitats in subtropical oceanic waters (Kashiwagi et al. 2011). Due to its large size and seasonal sightings, *M. birostris* has been proposed to be a highly nomadic and migratory species (Hearn et al. 2014, Couturier et al. 2015). However, site fidelity has been reported in specific locations such as the Revillagigedo Islands in Mexico and the Raja Ampat Archipelago in Indonesia (Stewart et al. 2016). The first studies conducted on *M. birostris* (Clark 2002, Marshall 2008, Dewar et al. 2008) pre-date its taxonomic separation from *M. alfredi* (Marshall et al. 2009), so in these publications, the information on these 2 species could be misleading. However, in this paper, when we refer to giant manta rays (*M. birostris*), we have only used studies published after the taxonomic separation.

The attraction of *M. birostris* to highly productive tropical and subtropical areas where some targeted species such as tuna aggregate, coupled with the giant manta ray's large size and distribution in epipelagic zones, have made it vulnerable to bycatch in fisheries (Stewart et al. 2018). This has led to population declines and the categorization of the species as Endangered in the IUCN Red List of Threatened Species (IUCN 2020). Although important conservation steps have been made, such as the inclusion of *M. birostris* in Appendix II of the Convention on International Trade in Endangered Species of Wild Fauna and Flora (CITES) (Marshall et al. 2011a,b), research is still needed to understand population structure and dynamics at local and regional scales, especially in key aggregation sites such as Isla de La Plata near the Ecuadorian coastline (Dulvy et al. 2014, Hearn et al. 2014, Kashiwagi et al. 2015) and the Galapagos Islands (Hearn et al. 2014, Lezama-Ochoa et al. 2019a). In highly mobile marine species, the identification of aggregation sites has proven useful for understanding critical biological processes (Derous et al. 2007, Lieber et al. 2020). In mobulids, aggregation sites have been linked to areas with high primary productivity, where individuals congregate mainly to forage and reproduce (Armstrong et al. 2016, Stewart et al. 2018). Characterization of the

populations that occur in these areas could provide insights into the giant manta ray's distribution, movements, and behavior (Stewart et al. 2018).

Genetic studies of *M. birostris* are limited worldwide (Stewart et al. 2016, Hosegood 2020), and none of these reports include samples from Ecuadorian oceanic waters. World information about giant manta rays has been predominantly gathered through diver counts, photo-identification surveys, and acoustic and satellite tags of targeted populations at aggregation sites (Stewart et al. 2018). Although this data has contributed to an understanding of the population dynamics of the species, genetic analyses are still needed to assess population structure and identify areas of overlap between mobulid hotspots and fisheries, which could ultimately help reduce their bycatch rates (Stewart et al. 2018). Moreover, genetic information (e.g. reduced genetic diversity) could provide insights into the risks and vulnerability associated with inbreeding or demographic changes and contribute to creating efficient conservation plans based on genetic assessments rather than directing efforts based on political or geographic boundaries (Milton & Shaklee 1987, Allendorf et al. 2010, Bester-van der Merwe & Gledhill 2015, Domingues et al. 2018, Stewart et al. 2018). In this sense, evaluating the genetic diversity of *M. birostris* could help prioritize vulnerable populations for conservation and management actions (Stewart et al. 2018).

Population structure and genetic diversity in marine environments can vary temporally due to several factors, such as climatic change, inner habitat characteristics, oceanic currents, geographic distances, biotic interactions, and early life history (Reynolds et al. 2017, Lassauce et al. 2022). Importantly, giant manta rays display site fidelity linked to resource availability, which is another key process that can shape population structure by limiting migration rates (Stewart et al. 2016, Lezama-Ochoa et al. 2019a). Specifically, planktivores rely on conditions influencing their environment, which shape the abundance and availability of their food sources (Burgess 2017, Lassauce et al. 2022). This, in turn, has been hypothesized as a driver for giant manta ray movements and migration (Stewart et al. 2016). Understanding how these factors may affect the populations present off the coast of mainland Ecuador and in the Galapagos is key to comprehending the ecology and behavior of the individuals present at these sites.

Given the favorable oceanic conditions (i.e. high productivity) during the summer off mainland Ecuador (July to October) and in the Galapagos (December to May) and the ability of *M. birostris* to perform long-

distance migration (Marshall et al. 2011a, Hearn et al. 2014, Andrzejaczek et al. 2021), we hypothesized that *M. birostris* individuals could migrate between these 2 locations during seasons of high primary productivity and that they might constitute a panmictic population. Therefore, the objective of this study was to assess the genetic diversity, population structure, and connectivity of *M. birostris* individuals sampled off mainland Ecuador and in Galapagos throughout the course of several sighting seasons.

2. MATERIALS AND METHODS

2.1. Sample collection and DNA extraction

A total of 148 *Mobula birostris* muscle/skin tissue samples were collected from free-swimming giant manta rays, using a biopsy tip mounted on a spear pole while SCUBA or free diving. Of these samples, 127 were collected off the coast of mainland Ecuador during the 2013−2018 sighting seasons from August to September (2013: n = 24; 2014: n = 26; 2015: n = 26; 2016: n = 11; 2017: n = 14; 2018: n = 26); 121 were collected at Isla de la Plata (located ~30 km from Manabi Province in mainland Ecuador) and 6 were collected from Bajo Cope (~65 km from Isla de la Plata). Both locations (Isla de la Plata and Bajo Cope) are hereafter referred to collectively as mainland Ecuador. The remaining 21 samples were collected from the Galapagos during the 2019 sighting season from March to June. Samples were stored in 96% ethanol until DNA extraction.

Sampling details and collection sites are provided in Table S1 in the Supplement at www.int-res.com/articles/suppl/m699p075_supp.pdf. Genomic DNA was extracted using a Proteinase K protocol described by Broderick et al. (2011). Maps of the georeferenced sampling sites on mainland Ecuador and Galapagos were drawn using ArcGIS Desktop 10.2 (ESRI 2020) (see Fig. 1).

2.2. Simple-sequence repeat amplification and genotyping

A total of 8 simple-sequence repeat (SSR) polymorphic microsatellite markers designed for *M. alfredi* (Kashiwagi et al. 2012) were used in this study. PCR reactions had a final volume of 25 µl, which included 1× PCR buffer (Invitrogen), 1.5−2.5 mM MgCl$_2$ (Invitrogen), 0.4 mM dNTPs (Invitrogen), 0.15 µM of tail A modified forward primer, 0.5 µM of reverse primer, 0.2 µM of tail A fluorescent primer, 0.1−1 mg ml^{-1} BSA, 1 U of *Taq* DNA polymerase (Invitrogen), and 10−20 ng of DNA. The thermocycling conditions consisted of an initial denaturation step at 94°C for 5 min, followed by 37 cycles (30 s at 94°C, 45 s at 55−65°C, 72°C for 1.5 min) with a final extension step of 10 min at 72°C (Kashiwagi et al. 2012 with modifications). PCR products from the 2014−2019 seasons were labeled with one of 4 fluorescent dyes (6-FAM, VIC, PET, or NED), using universal primers in a 3-primer system described by Blacket et al. (2012). Labeled amplified PCR products were genotyped by Macrogen on an ABI 3130 Genetic Analyzer (Applied Biosystems) automatic capillary sequencer, using 500LIZ as a size standard. Genotyping results were analyzed using the software GeneMarker v.2.4.0 (Softgenetics).

Samples for the 2013 season were genotyped via polyacrylamide gel electrophoresis: PCR products were separated using 6% polyacrylamide gels, and gels were revealed using the silver staining protocol as described by Benbouza et al. (2006). Amplicon size for each allele was calculated using linear regression with a 100 bp ladder (Invitrogen). For standardizing the allele sizes obtained by polyacrylamide electrophoresis with the ones obtained by fluorescence genotyping, 15 bp corresponding to the universal 5′ tail was added to the final amplicon size.

2.3. Relatedness analysis

Relatedness between individuals and within seasons was examined using the R package 'related' v.1.0 (Pew et al. 2015) in R v.3.6.2 (R Core Team 2019). This program calculates relatedness from microsatellites using 7 different estimators (Pew et al. 2015). To test the performance of the estimators, we calculated the Pearson correlation coefficient between observed and expected relatedness for each case. Based on these results, we chose to use the Wang estimator for relatedness analysis (Wang 2002).

To account for the possibility that the same individual might have been resampled multiple times within a season, we performed pairwise comparisons among individuals and then randomly eliminated one individual from each pairwise comparison that showed high relatedness values ($R > 0.7$). Based on the allele frequencies of the data set, we performed simulations of 100 individuals with a predefined degree of relatedness. We then calculated the pairwise relatedness values among all sampled individuals and clas-

sified them into specific relatedness groups. Relatedness indexes among seasons were statistically compared by 1-way ANOVA. We also conducted 1000 Monte Carlo simulations (1000 iterations) to calculate the expected relatedness distribution in each season.

2.4. Genetic diversity estimation

Genetic diversity parameters such as the number of alleles per locus (N_a), polymorphic information content (PIC), expected heterozygosity (H_e), observed heterozygosity (H_o), and inbreeding coefficient (F) were calculated with the R package 'adegenet' v.2.1.3 (Jombart 2008).

Confidence intervals for H_e were calculated with the R package 'PopGenKit' v.1.0. MicroDrop v.1.01 (Wang & Rosenberg 2012) was run on the pooled data set using default parameters to evaluate allelic dropout rates across all loci. Allelic richness was calculated using the R package 'POPGENREPORT' v.3.0.4 (Adamack & Gruber 2014). The number of private alleles (N_{pa}) was determined with the R package 'poppr' (Kamvar et al. 2014). N_a, allelic richness R_s, and N_{pa} were also calculated through rarefaction by standardizing to the minimum sample size with the R package 'diveRsity' v.1.9.90 (Keenan et al. 2013). Null allele (N_o) frequencies for each locus were obtained using 'FreeNA' (Chapuis & Estoup 2007), considering the expectation maximization (EM) algorithm. Given the fact that N_o can bias population structure analysis, corrected pair-wise fixation index (F_{ST}) values were compared to uncorrected values using the excluding N_o (ENA) method with a paired t-test. Deviations from Hardy-Weinberg equilibrium (HWE) were calculated in GENEPOP v.4.2 (Raymond & Rousset 1995).

2.5. Evaluation of population structure

F_{ST} was calculated by running an analysis of molecular variance (AMOVA) in ARLEQUIN v.3.5.2.2 (Excoffier & Lischer 2010) with significance tested against 10 000 permutations. The AMOVA significance level was adjusted to $\alpha = 0.05$. A principal coordinate analysis (PCoA) was performed using the 'ape' v.5.4-1 package (Paradis & Schliep 2019) and plotted with ggplot2 v.3.3.3 (Wickham 2009) to visualize the genetic structure between Galapagos and mainland Ecuador and among seasons within mainland Ecuador. Population structure was inferred through a Bayesian individual-based clustering approach using STRUC-TURE v.2.3.4 (Pritchard et al. 2000). The number of clusters was determined using an admixture model, where K values between 1–10 were evaluated, considering 5 iterations for each K value. Each run consisted of 1 000 000 Markov chain Monte Carlo (MCMC) iterations with a 100 000 step burn-in period. The optimal K value was obtained using the Evanno method (Evanno et al. 2005) implemented in STRUC-TURE HARVESTER (Earl & von Holdt 2012), and information corresponding to all individual runs was compiled using CLUMPP (Jakobsson & Rosenberg 2007). The final STRUCTURE plot was obtained using the software 'Distruct' (Rosenberg 2003).

2.6. Migration analysis

To investigate directional gene flow and its relative magnitude among the different seasons of *M. birostris* in mainland Ecuador and the Galapagos, we used the R package 'diveRsity' v.1.9.90 (Keenan et al. 2013). This method computes migration rates between all sites and then normalizes them to obtain relative migration rates that vary between 0 and 1. Computations were performed using effective number of migrants ($N_{mAlcala}$), which is a statistic introduced by Alcala et al. (2014) (Sundqvist et al. 2016). This statistic uses the genetic differentiation measures G_{ST} and D to estimate $N_{mAlcala}$, from which the relative migration rate is calculated.

2.7. Compilation of environmental oceanographic data

To further describe the variables associated with both sampling locations, information corresponding to oceanographic conditions during the sampling periods was collected from 2 online databases. The data was downloaded from the EU Copernicus Marine Environment Monitoring Service (CMEMS; http://marine.copernicus.eu) and Environmental Research Division's Data Access Program (ERDDAP; https://www.ncei.noaa.gov/erddap/index.html). CMEMS is a platform that gathers information from multiple databases on the ocean's state, variability, and dynamics from marine ecosystems around the world (von Schuckmann et al. 2016, Lezama-Ochoa et al. 2019b). ERDDAP is a data server that grants access to scientific data sets on oceanographic data collected from satellites and buoys around the world (Simons 2020). The following environmental variables were downloaded: daily sea surface temperature (SST; °C),

monthly chlorophyll *a* (chl *a*; mg m^{-3}), and monthly oxygen concentration (O$_2$; mmol m^{-3}). All variables were collected at a 0.25° spatial resolution using python routines and motuclient from CMEMS and a 0.025° spatial resolution from ERDDAP. These variables were selected since they are considered indicators of primary productivity levels associated with aggregation areas for giant manta rays (Lezama-Ochoa et al. 2019a).

3. RESULTS

3.1. Relatedness

A total of 148 *Mobula birostris* samples were collected and genotyped from mainland Ecuador (n = 127) during 6 consecutive seasons (2013–2018), and from southwest Galapagos (n = 21) during one season (2019) (Fig. 1). In order to avoid biased estimations of genetic diversity and population structure, a relatedness analysis was conducted to exclude related individuals from further analysis. The results from this analysis showed 2 pairs of duplicate individuals ($R = 1$) and 10 pairs of highly related individuals ($R > 0.7$). One individual from each pair was randomly removed from the data set (4 from 2013, 1 from

2014, 1 from 2015, 1 from 2016, 2 from 2018, and 3 from 2019). Therefore, all remaining analyses were performed on a data set of 136 individuals (118 from mainland Ecuador and 18 from Galapagos).

Monte Carlo simulations indicated that the relatedness observed for individuals for the 2013, 2014, 2018, and 2019 seasons was significantly higher (p < 0.001) than would be expected by random mating, meaning that individuals from these seasons are more closely related than expected by chance (Fig. S1). According to the Monte Carlo simulations, giant manta rays from the same seasons (2013, 2014, 2018, and 2019) presented a higher median Wang relatedness value (middle line in the box plot in Fig. S2) compared to individuals from 2015, 2016, and 2017. Significant differences (p < 0.05) in relatedness indexes among the aforementioned seasons were found by 1-way ANOVA.

Analysis among seasons indicated that the Wang median value was higher when considering only individuals from mainland Ecuador (seasons 2013–2018) than when comparing all individuals from both localities (2013–2019). This finding indicates that there was a higher number of related individuals in the samples collected only in mainland Ecuador than when samples from Galapagos were included (Fig. S2).
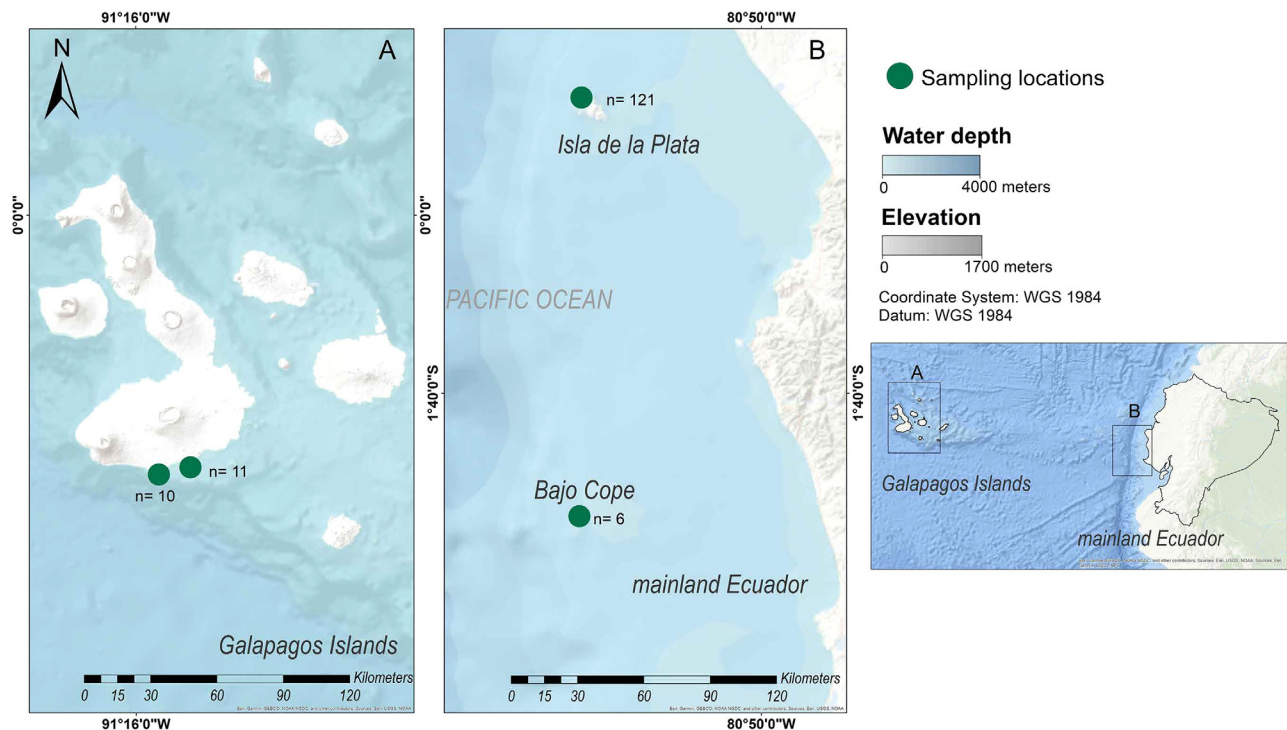

Fig. 1. *Mobula birostris* sample collection sites off mainland Ecuador and in the Galapagos Islands. Green dots: collection sites; number of samples is displayed next to each dot. This map was drawn using ArcGIS Desktop v.10 (ESRI 2020)

3.2. Genetic diversity

The data set of 136 individuals was genotyped at 8 microsatellite loci. The mean N_o frequency was 10.13%. Paired t-tests indicated no significant difference (p > 0.05) between uncorrected and corrected F_{ST} values, which indicates that N_o likely had no effect on the genetic analyses. All 8 loci were used in subsequent analyses. Allelic dropout was distributed between 0 and 20% across the 8 analyzed loci (0%: MA14; 20%: MA15). All markers deviated significantly (p < 0.05) from HWE by having less H_o than expected, except for locus MA09 (p = 0.64) (Sharma et al. 2016, Chen et al. 2017). A total of 94 alleles, ranging from 7–25 alleles per locus, were found in the data set. Furthermore, the PIC indicated that MA30 was the most informative marker, with a total of 25 alleles and a PIC value of 0.90. H_e ranged from 0.49 (MA21) to 0.90 (MA30) per locus, with a mean of 0.74. A summary of the overall genetic diversity per locus across the 136 individuals is provided in Table 1.

Overall genetic diversity varied among the 6 seasons in mainland Ecuador. The average N_a per season ranged from 47 (2013) to 58 (2015), and N_{pa} ranged from 1 allele (2016) to 4 alleles (2014 and 2017).

The highest H_e was found in 2015 (0.74) and the lowest in 2013 (0.61). Allelic richness estimates showed little difference across the data. The highest values of F were observed in 2015 (0.24) and 2017 (0.22); the lowest F was found in 2016 (0.01). A higher degree of genetic diversity was obtained in mainland Ecuador (H_e = 0.72) in comparison to the Galapagos (H_e = 0.66). Allelic richness estimates were also higher for mainland Ecuador (7.15) than Galapagos (5) (Table 2).

3.3. Population differentiation and population structure

Genetic differentiation based on pairwise F_{ST} estimates between the 6 sighting seasons for mainland Ecuador indicated that the greatest differentia-

Table 1. Genetic diversity estimates for *Mobula birostris* obtained for each simple-sequence repeat (SSR) marker, including number of alleles (N_a), allele dropout (ADO), expected heterozygosity (H_e), observed heterozygosity (H_o), polymorphic information content (PIC), null allele frequency (N_o), F_{st} without using the ENA correction for null alleles ($F_{ST}{}^A$), F_{st} using the ENA correction for null alleles ($F_{ST}{}^B$), and deviation from Hardy-Weinberg Equilibrium (HWE) p-value

SSR marker	N_a	ADO	H_e	H_o	PIC	N_o	$F_{ST}{}^A$	$F_{ST}{}^B$	HWE
MA09	8	0.00	0.62	0.61	0.57	0.00	0.01	0.01	0.64
MA14	13	0.00	0.81	0.72	0.79	0.06	0.03	0.03	0.00
MA15	11	0.19	0.82	0.47	0.80	0.20	0.08	0.06	0.00
MA21	7	0.14	0.49	0.21	0.46	0.21	0.05	0.05	0.00
MA30	25	0.15	0.90	0.65	0.90	0.12	0.09	0.10	0.00
MA34	8	0.00	0.60	0.55	0.57	0.05	0.07	0.07	0.00
MA43	8	0.02	0.81	0.62	0.79	0.11	0.10	0.11	0.00
MA49	14	0.00	0.83	0.72	0.81	0.07	0.08	0.08	0.00

Table 2. Genetic diversity estimates for *Mobula birostris* grouped by seasons in mainland Ecuador and by location in mainland Ecuador and Galapagos. Number of individuals (N), number of alleles (N_a), number of alleles with rarefaction (N_a rarefaction), expected heterozygosity (H_e), observed heterozygosity (H_o), number of private alleles (N_{pa}), number of private alleles with rarefaction (N_{pa} rarefaction), allelic richness (R_s), allelic richness with rarefaction (R_s rarefaction), and inbreeding coefficient (F) using the Ritland method (Ritland 2009)

	N	N_a	N_a rarefaction	H_e	H_o	N_{pa}	N_{pa} rarefaction	R_s	R_s rarefaction	F
Seasons										
2013	20	46	47	0.61	0.6	3	3	4.65	5.01	0.06
2014	25	57	54	0.68	0.56	5	4	5.24	5.44	0.13
2015	25	60	58	0.74	0.55	3	3	5.78	5.99	0.24
2016	10	53	53	0.71	0.66	1	1	5.91	6.63	0.01
2017	14	56	56	0.69	0.53	4	4	5.80	6.26	0.22
2018	24	58	55	0.63	0.47	2	2	5.01	5.24	0.15
Locations										
Mainland Ecuador	118	90	66	0.72[a]	0.55	54	37	6.66	7.15	0.22
Galapagos	18	40	40	0.66[b]	0.7	4	8	4.59	5	0.01

[a]Upper bound: 0.74; lower bound: 0.70 of the H_e (mainland Ecuador) 95% CI
[b]Upper bound: 0.67; lower bound: 0.60 of the H_e (Galapagos) 95% CI

tion occurred between 2018/2013 as well as 2018/ 2014 (F_{ST} = 0.08, p < 0.05 for both comparisons); whereas the lowest genetic distance was found between 2017/2014, 2017/2015, and 2017/2016 (F_{ST} = 0.01 for all comparisons; p = 0.33, 0.53, and 0.31 respectively) (Table 3). When comparing mainland Ecuador to Galapagos, the F_{ST} index revealed significant genetic differentiation (F_{ST} = 0.08, p < 0.05).

A PCoA based on genetic distances suggested that the first 2 principal components accounted for 10.35 and 7.48% of the genetic variation in the 136 *M. birostris* individuals, together explaining 17.83% of the total variation. The PCoA plot revealed 2 clusters, one grouping the Galapagos samples and the other grouping samples from mainland Ecuador. However, a few individuals were included in both clusters (Fig. 2). A PCoA performed only on the samples from mainland Ecuador comparing seasons (Fig. S3) suggested no clear population structure (2013–2018). Overall, the PCoA plotting analysis comparing mainland Ecuador and Galapagos illustrated a pattern consistent with the obtained pairwise F_{ST} values, suggesting the possibility that these are 2 genetically different populations.

The STRUCTURE clustering analysis for all samples (2013–2019) tested *K* values ranging from 1–10 (Fig. S4). Results from *K* = 2 to *K* = 10 indicated differentiation between lineages from mainland Ecuador (2013–2018) and Galapagos (2019) (Fig. S4). In addition, the *K* = 3 and *K* = 5 graphs showed different genetic lineages between mainland individuals from the 2013 and 2018 seasons as well as the rest of the mainland Ecuador seasons (2014–2017) (Fig. S4), which was also supported by F_{ST} values (Table 3). According to the Evanno method, the optimal Δ*K* value is 3, supporting the presence of 3 genetic lineages: 2 corresponding to mainland Ecuador (purple and blue bars in Fig. 3a) and one corresponding to Galapagos (orange bars in Fig. 3a).

The STRUCTURE analysis for the different seasons in mainland Ecuador (2013–2018) also tested *K* values from 1–10 (Fig. S5). In this case, the *K* = 2 and *K* = 4 graphs once again indicated a difference in the composition of the genetic lineages between individ-

Table 3. Pairwise F_{ST} values (above the diagonal) between 6 sighting seasons from mainland Ecuador of *Mobula birostris* (118 sampled individuals) and between mainland Ecuador and Galapagos (18 sampled individuals) as revealed by the microsatellite dataset (8 loci), and the corresponding p-values (below the diagonal); significant p-values are in bold, and p-values of 0.00 signify a p-value < 0.005

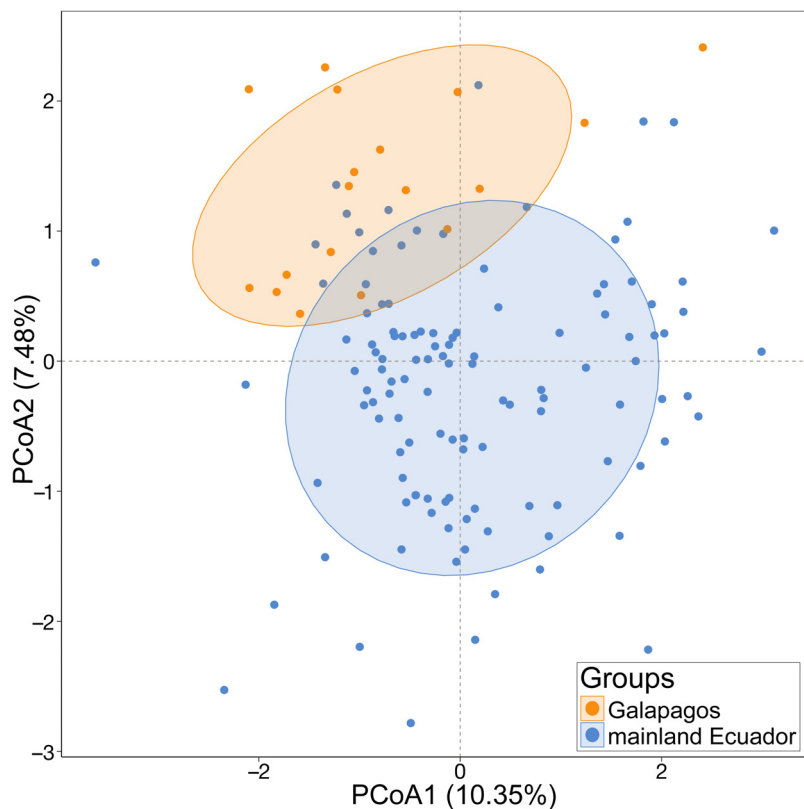|	Mainland Ecuador	Galapagos	2013	2014	2015	2016	2017	2018
Mainland Ecuador	–	0.08						
Galapagos	**0.00**	–						
2013			–	0.06	0.07	0.05	0.04	0.08
2014			**0.00**	–	0.02	0.04	0.01	0.08
2015			**0.00**	**0.02**	–	0.02	0.01	0.04
2016			**0.00**	**0.00**	0.19	–	0.01	0.05
2017			**0.00**	0.33	0.53	0.31	–	0.05
2018			**0.00**	**0.00**	**0.00**	**0.01**	**0.00**	–

Fig. 2. Principal coordinate analysis (PCoA) based on the Euclidian genetic distances of *Mobula birostris* (n = 136) using 8 SSR markers. The first 2 components represent 17.8% of the total variation. Two genetic clusters were found corresponding to mainland Ecuador and Galapagos. Ellipses: 95% CIs
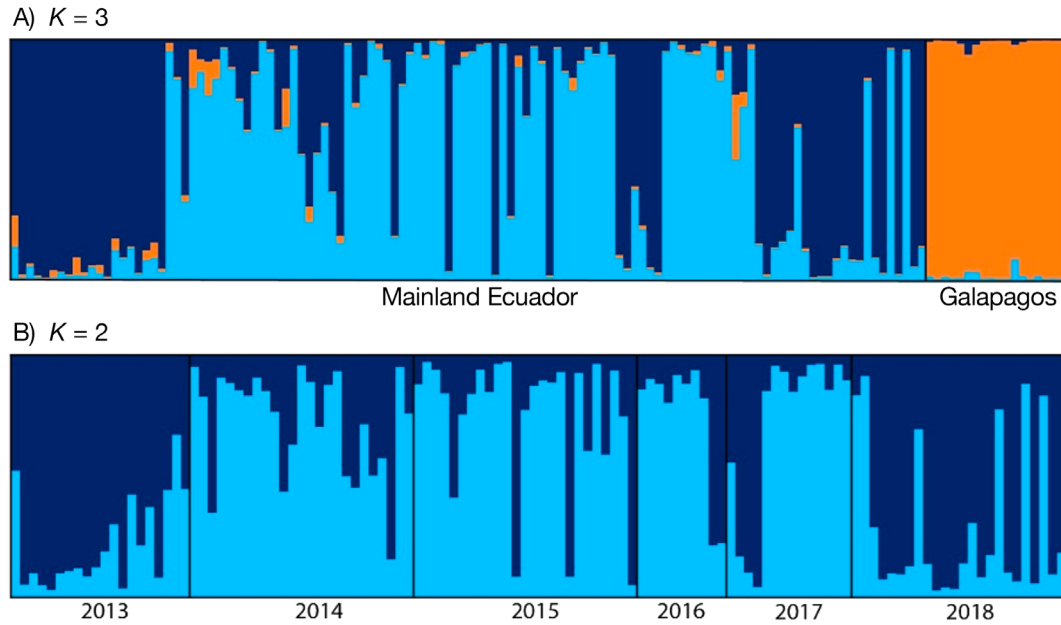
Fig. 3. Bayesian analysis of population structure under the admixture model for *Mobula birostris* using 8 SSR markers. Each vertical bar represents one individual, and the color proportion for each bar corresponds to the probability of assignment of each individual to a different lineage (K). (A) Comparison between individuals of mainland Ecuador and Galapagos (n = 136) at $K = 3$; (B) Comparison between the 6 sighting seasons in mainland Ecuador (n = 118) at $K = 2$

uals from the 2013 and 2018 seasons as well as with individuals from the rest of the mainland Ecuador sighting seasons (2014–2017) (Fig. S5). For these analyses, the Evanno method revealed that the highest K value was 2, implying the presence of 2 lineages (Fig. 3b). The 2013 and 2018 seasons are characterized by a higher proportion of one genetic lineage (purple bars in Fig. 3b; average proportion: 0.742), while the 2014–2017 seasons are characterized by a higher proportion of the other genetic lineage (blue bars in Fig. 3b; average proportion: 0.734).

3.4. Gene flow and relative migration between mainland Ecuador and Galapagos

The migration networks revealed different levels of migration rates and gene flow within 2013–2018 in mainland Ecuador, and between these years and the single sighting season (2019) in Galapagos. The relative migration network (Fig. 4) showing migration rates above 0.4 revealed the strongest bidirectional gene flow (0.52–0.88) between seasons 2014–2017. Individuals from 2018 exhibited a relatively low bidirectional gene flow (0.44–0.57) with individuals from 2014–2017.

To further analyze the limited gene flow between 2013 and 2019 (Galapagos) with the rest of the seasons from mainland Ecuador (2014–2018), we cre-

ated a network displaying a migration rate threshold of 0.1, which presents the lowest unidirectional gene flow (0.12) between Galapagos (2019) and mainland Ecuador for the rest of the seasons (2014–2018) (Fig. S6). Together, these results (F_{ST} indexes, PCoA, STRUCTURE, and migration analyses) support the presence of 2 separate populations: one in mainland Ecuador and one in the Galapagos, refuting the single panmictic population hypothesis.

3.5. Environmental characteristics at the sampling locations associated with giant manta ray aggregation

To understand how environmental characteristics could be contributing to the presence of 2 distinct populations in Ecuadorian waters, oceanographic variables were gathered for mainland Ecuador and Galapagos for the 2013–2019 seasons (Table 4). During this period, average chl *a* concentrations ranged from 0.54 to 1.20 mg m^{-3} in mainland Ecuador and 0.26 to 0.56 mg m^{-3} in Galapagos; SSTs ranged from 23.97 to 25.18°C in mainland Ecuador and 23.16 to 25.43°C in Galapagos; and O$_2$ concentrations ranged from 216.39 to 219.42 mmol m^{-3} in mainland Ecuador and 216.06 to 218.93 mmol m^{-3} in Galapagos (Table 4). All ranges observed for these variables are congruent with conditions previously reported for the occurrence,
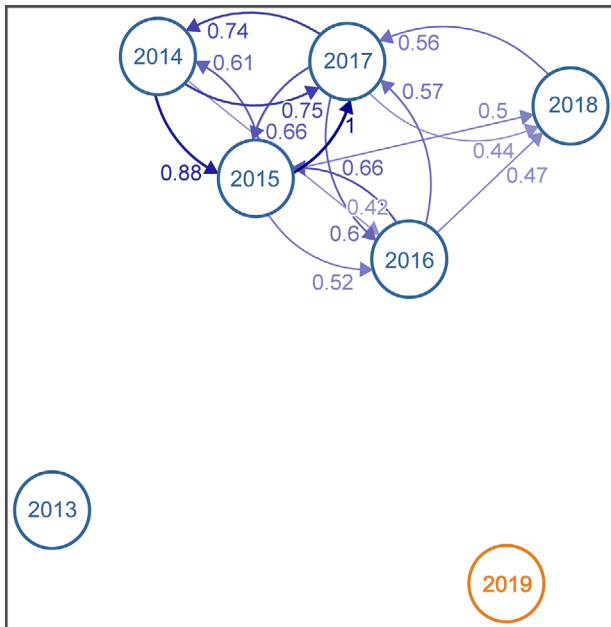
Fig. 4. Relative migration network diagram for *Mobula birostris* corresponding to the 6 sighting seasons (2013–2018; blue) in mainland Ecuador and Galapagos (2019; orange). The network was visualized with 'divMigrate' using Alcala's $N_{mAlcala}$ (see Section 2.6), with relative migration rates below 0.40 filtered out. Line shading and thickness are proportional to the relative migration rate between groups. Numbers indicate gene flow rate, scaled from 0 to 1

preference, and aggregation of *M. birostris* (Anderson et al. 2011, Graham et al. 2012, Lezama-Ochoa et al. 2019a, Putra et al. 2020, Farmer et al. 2022).

4. DISCUSSION

In this study, we examined the genetic composition of *Mobula birostris* in 2 important aggregation zones of the Eastern Tropical Pacific and shed light on its population structure and distribution — key factors for the conservation of this Endangered marine species. Based on F_{ST}, population structure, and migration analyses, our results suggest the presence of 2 different populations of giant manta rays, with reduced/limited gene flow between mainland Ecuador and Galapagos.

4.1. Genetic status of *M. birostris* in 2 aggregation zones in the Eastern Pacific

Moderately high levels of genetic diversity were found in mainland Ecuador and the Galapagos (H_e = 0.72 and H_e = 0.66, respectively). To the best of our

knowledge, no previous studies have evaluated the genetic diversity of *M. birostris* using SSR markers, but these values are comparable to or higher than those reported for other elasmobranchs, such as whale sharks collected worldwide (H_e = 0.68) (Schmidt et al. 2009), white sharks from South Africa (H_e = 0.66) (Pardini et al. 2000), and closely related species such as the reef manta ray from Japan (H_e = 0.48) (Kashiwagi et al. 2012).

The only other study evaluating genetic diversity in *M. birostris* was conducted by Hosegood (2020), who used single nucleotide polymorphism (SNP) markers from individuals sampled from 7 locations worldwide and reported low levels of genetic diversity (H_e = 0.06). However, the data from Hosegood (2020) is not comparable to our study due to both the inner characteristics of the molecular markers used (SNPs: genome-wide analyzed loci; SSRs: specific analyzed loci) (Fischer et al. 2017) and the difference in sampling strategy: our sample size was larger (Hosegood 2020: n = 99; this study: n = 136) and we sampled manta rays from a much smaller geographic area that had not been previously studied.

The moderately high genetic diversity we found could be the result of the aggregation of a large number of individuals in the studied locations. Isla de la Plata off mainland Ecuador hosts one of the largest populations of *M. birostris* in the world (a total of 2400 individuals), compared to other populations reported in Pacific Mexico (n = 715) and Raja Ampat in Indonesia (n = 588) (Beale et al. 2019, Palomino et al. 2020). In general, larger populations tend to show higher levels of genetic diversity, mainly because of a higher likelihood of maintaining a robust genetic pool (Yun et al. 2020). In addition, the Galapagos and mainland Ecuador have been reported as important habitat and aggregation sites for this species (Vergara-Chen et al. 2015, Lezama-Ochoa et al. 2019a,b). Aggregation sites have been found to foster encounters and interbreeding between individuals that may come from genetically distinct stocks. Such events could help explain the increased genetic diversity indexes obtained for giant manta rays at these locations, as has been previously reported for green sea turtles in the Atlantic (Vásquez-Carrillo et al. 2020).

For species such as *M. birostris*, where population declines have been reported, it is important to determine parameters such as genetic diversity and connectivity (Beale et al. 2019, Sandoval-Castillo 2019, Hosegood 2020). A decreasing population usually loses diversity due to inbreeding, excessive genetic drift, and population fragmentation, which in turn

Table 4. Oceanographic variables obtained from Copernicus Marine Environment Monitoring Service (CMEMS) and Environmental Research Division's Data Access Program (ERDDAP); (–) values not reported

Database ID	Oceanographic variable	Variable name	Units	Spatial resolution	Temporal resolution		2013	2014	2015	2016	2017	2018	2019
Mainland Ecuador													
NOAA_DHW_monthly	Temperature	Sea surface temp	°C	0.0025°	Monthly	Max.	26.43	26.55	27.59	27.46	28.83	27.53	–
						Av.	23.97	24.47	25.18	25.18	25.09	24.20	24.71
						Min.	19.66	20.12	21.54	19.13	20.06	20.83	–
pmlEsaCCI31OceanColorMonthly	Chlorophyll a	chlor_a	mg m^{-3}	0.0025°	Monthly	Max.	11.38	8.35	10.75	10.41	8.92	–	–
						Av.	0.74	0.77	0.73	0.64	0.54	–	–
						Min.	0.08	0.03	0.06	0.01	0.06	–	–
nesdisVHNSQchlaDaily				0.0025°	Daily	Max.	–	–	–	–	–	99.67	98.38
						Av.	–	–	–	–	–	1.10	1.20
						Min.	–	–	–	–	–	0.06	0.07
GLOBAL_REANALYSIS _BIO_001_029-TDS_daily	Oxygen	O$_2$	mmol m^{-3}	0.025°	Daily	Max.	229.79	223.87	220.64	221.87	225.67	228.95	229.68
						Av.	219.42	217.64	217.24	216.47	216.39	218.03	216.88
						Min.	213.94	212.42	211.79	210.98	210.48	209.68	207.99
Galapagos													
NOAA_DHW_monthly	Temperature	Sea surface temp	°C	0.0025°	Monthly	Max.	27.49	27.44	28.64	28.36	28.64	27.24	–
						Av.	23.16	24.32	25.43	24.22	23.53	23.52	23.8
						Min.	18.37	19.61	21.04	18.56	17.28	18.22	–
pmlEsaCCI31OceanColorMonthly	Chlorophyll a	chlor_a	mg m^{-3}	0.0025°	Monthly	Max.	13.57	4.50	10.28	7.82	8.72	–	–
						Av.	0.36	0.31	0.26	0.34	0.34	–	–
						Min.	0.08	0.04	0.05	0.05	0.05	–	–
nesdisVHNSQchlaDaily				0.0025°	Daily	Max.	–	–	–	–	–	96.07	97.28
						Av.	–	–	–	–	–	0.42	0.56
						Min.	–	–	–	–	–	0.08	0.07
GLOBAL_REANALYSIS _BIO_001_029-TDS_daily	Oxygen	O$_2$	mmol m^{-3}	0.025°	Daily	Max.	240.45	238.85	236.85	238.54	238.63	238.08	232.91
						Av.	217.90	218.64	218.30	218.93	217.47	217.66	216.06
						Min.	181.36	210.15	209.35	210.05	209.27	208.93	208.58

diminishes the species' capacity to adapt (Allendorf et al. 2010, Torres & Gutiérrez 2018). Despite reports indicating that *M. birostris* may be declining worldwide, populations in Ecuadorian waters appear to be stable and moderately diverse. These results could be important for *M. birostris* management and conservation (Hook 2017, Sandoval-Castillo 2019).

It is important to note the limitations of the present study with respect to estimation of genetic diversity and inference of population structure due to the number of samples analyzed in some seasons (2016 = 10 samples; 2017 = 14 samples) and because of the type and number of markers used (8 SSR markers). It has been suggested that at least 30 individuals per population are necessary for population genetic analysis (Putman & Carbone 2014, Danusevicius et al. 2016); however, this number cannot always be reached, especially when working with species such as *M. birostris*, where sampling is challenging. In addition, Putman & Carbone (2014) suggested that ideally >50 SSRs would be needed to obtain good resolution of a species' population structure, whereas other reports state that correct assignment of individuals to their specific clusters can be obtained with as few as 8 markers (Arthofer et al. 2018). Nevertheless, further studies should consider increasing the number of loci analyzed and the number of samples per locality to obtain a more accurate estimate of the genetic diversity and population structure of this species.

4.2. Population structure and connectivity

A combination of F_{ST} indexes, PCoA analysis, Bayesian population structure modeling, and migration networks suggest the presence of 2 discrete populations of *M. birostris* in mainland Ecuador and Galapagos (~1000 km apart). Similarly, Stewart et al. (2016) used SNP markers and revealed well-structured giant manta ray subpopulations in Coastal Mexico (Bahía de Banderas), offshore Mexico (Revillagigedo Islands), and Sri Lanka. However, Hosegood (2020) reported a lack of differentiation and population structure between distant locations from around the world (Mexican Pacific, Mexican Caribbean, South Africa, Sri Lanka, Phillipines, and Peru), using SNPs. Differences between both studies can be explained by the contrasting analytic strategies used with their data sets. Importantly, the study by Hosegood (2020) did not include samples from Ecuador. The presence of discrete groups in a previously unstudied area highlights the need to fill geographic gaps and to understand the genetic structure of *M. birostris* globally.

Migration patterns of *M. birostris* in the Eastern Pacific have been analyzed recently using satellite tags and acoustic devices and suggest few exchanges of individuals and sporadic large-scale movements (Hearn et al. 2014, Palomino et al. 2020, Andrzejaczek et al. 2021). Palomino et al. (2020) tagged 46 giant manta rays at Isla de la Plata (near Manabi Province in mainland Ecuador) with acoustic devices (n = 30) and satellite tags (n = 16). Most of the giant manta rays displayed high residency within the study area (moving less than 95.3 km), whereas a few individuals migrated south towards Peruvian waters (387 km). More recently, Andrzejaczek et al. (2021) found that 2 tagged individuals moved north along the coast of Ecuador from Tumbes to other sites such as Isla de la Plata (263 km), and a third individual performed a large-scale movement from Peru to northern Ecuador and then traveled in a westerly direction to the Galapagos Islands (approximately 1300 km). Importantly, the satellite data for this third individual shows that it stayed within the Galapagos Marine Reserve for less than 1 mo in September 2018 before moving in a southeastern direction. This differs from local observations in southern Galapagos, where giant manta rays are commonly seen from December to June (D. Pazmiño pers. comm.). Hearn et al. (2014) also reported that one out of 9 tagged individuals moved from Isla de la Plata to the Galapagos Islands. Despite evidence of single individuals migrating between locations, the limited gene flow found in this study between mainland Ecuador and Galapagos (Figs. 4 & S6) is not surprising since large populations usually have low genetic drift and require very low migration rates to maintain genetic similarity even if they have become physically separated (Veríssimo et al. 2017, Marandel et al. 2018). The 2 tagged individuals that migrated between mainland Ecuador and Galapagos in 2012 and 2018 (Hearn et al. 2014, Andrzejaczek et al. 2021) could indicate genetic connectivity among these populations, since in order to establish this kind of connectivity it would be necessary to find at least one migrant for every 10 generations. For *M. birostris*, which has an approximate generation time of 25 yr, these 2 migration events could be sufficient to establish genetic connectivity between these 2 populations (Lowe & Allendorf 2010, Marshall et al. 2011a, Marandel et al. 2018). Notwithstanding, without knowing the reproductive status of these 2 marked individuals it would be difficult to establish any conclusions about the connectivity between these populations. Thus, the limited connectivity found in this study may be associated with a resident behavior of *M. birostris* at the sampling locations. Such behavior has also been re-

ported for *M. birostris* in Mexican waters, where a defined population structure was found between Bahia de Banderas and Revillagigedo Island (distance ~ 600 km) (Stewart et al. 2016).

Palomino et al. (2020) and Andrzejaczek et al. (2021) suggested that the residence patterns and spatial–temporal variations in vertical movement observed for giant manta rays moving from Peru to Ecuador and vice versa could be associated with high primary productivity (in southeast Pacific coasts) and higher zooplankton biomass during the austral spring months. Stewart et al. (2016) postulated that with a year-round food source, a suitable juvenile habitat of *M. birostris* overlapping with adult habitat might eliminate incentives for long-range migratory behavior. Other highly migratory elasmobranchs, such as tiger sharks, have shown philopatric and residency behavior in the Galapagos associated with year-round reliable food sources (Acuña-Marrero et al. 2017). Thus, favorable oceanographic conditions found in Ecuadorian waters can influence spatial patterns of residency between mainland Ecuador and Galapagos populations by providing suitable habitat and a continuous food source in both locations, and by reducing the need for long-distance travel to feed.

In mainland Ecuador, the cold Humboldt Current induces upwelling of cold, nutrient-rich waters throughout the year. In the Galapagos, the convergence of the Panama, Humboldt, and Cromwell currents bring nutrient-rich waters to the northern, central, and western parts of the archipelago (Seminoff et al. 2008, Lezama-Ochoa et al. 2019a). The distinct oceanic currents in the Galapagos and around mainland Ecuador result in high productivity in both areas (Lezama-Ochoa et al. 2019a). Data from CMEMS and ERDDAP showed that the environmental variables in Isla de la Plata and Galapagos between 2013 and 2019 (SST: 23.16–25.43°C; chl *a*: 0.26–1.20 mg m^{-3}; [O_2]: 216.06–219.42 mmol m^{-3}) were similar to previously reported values for areas of high primary productivity where *M. birostris* tend to aggregate (SST: 20–30°C; chl *a*: 0.14–0.76 mg m^{-3}; [O_2]: 193.6–252.1 mmol m^{-3}; Anderson et al. 2011, Graham et al. 2012, Lezama-Ochoa et al. 2019a, Putra et al. 2020, Farmer et al. 2022), supporting the hypothesis that given favorable oceanographic conditions, giant manta rays prefer to stay rather than travel long distances.

We suggest that the genetic differentiation found among seasons (2013–2018 in relation to 2014–2017) in mainland Ecuador could be partially explained by fluctuations in temperatures and prey availability during phenomena like the El Niño–Southern Oscillation (ENSO) climate pattern (Osgood et al. 2021).

Seasons 2013 and part of 2018 were characterized by a strong coastal La Niña event, in contrast to the El Niño event reported for 2014–2016 (IMARPE 2021). La Niña is an oceanic and atmospheric phenomenon that is the colder counterpart of El Niño. During El Niño, winds that blow warm water from the Ecuadorian Pacific towards the Asian Pacific die down; at the same time, the influx of the Antarctic Humboldt Current, which brings cold water to the equator, is reduced (Montecino & Lange 2009, Edgar et al. 2010, Grados et al. 2018). The combination of these 2 events prevents the upwelling of cold and nutrient-rich deep ocean water towards the surface. This, in turn, starves primary levels of the food chain, hindering ocean production in general (Echevin et al. 2011, Grados et al. 2018). This process is particularly important for mobulid rays, as it has been suggested that gradual shifts in temperature could influence distributional changes since mobulids tend to track spatial changes in prey availability and are prone to migrate to areas with high primary productivity (Burgess 2017, Moreno & Gonzalez-Pestana 2017, Beale et al. 2019, Lezama-Ochoa et al. 2019 a,b, Osgood et al. 2021). We suggest that this could lead to the movement of individuals (which could belong to different populations) into areas where they have not been previously recorded and promote genetic exchange of individuals from distinct populations (Moreno & Gonzalez-Pestana 2017, Beale et al. 2019, Vásquez-Carrillo et al. 2020). It is important to highlight the need for further studies to better understand the influence of ENSO on the genetic composition of *M. birostris*.

5. CONCLUSIONS

Our study is a significant step toward a better understanding of the genetic diversity and population structure of *Mobula birostris* in important aggregation sites in mainland Ecuador and Galapagos. Results suggest a low migration rate between these 2 locations, which could be explained by a lack of long-distance (>1000 km) movement by *M. birostris* individuals given the favorable oceanographic conditions at each site. In particular, the permanent upwelling systems associated with the presence of Humboldt, Panama, and Cromwell currents in these 2 areas may influence the spatial and genetic composition of *M. birostris*, a filter-feeding organism that is known to chase ephemeral boosts of productivity (Hearn et al. 2014).

The well-defined genetic structure found in giant manta rays between Galapagos and mainland Ecuador

suggests that individuals from these 2 locations form separate populations, and the limited gene flow between the 2 aggregation sites does not support the idea of a panmictic population in Ecuadorian waters. This information is important to delimit appropriate management units that should be monitored and managed separately in *M. birostris* conservation (IUCN 2020). Moreover, this information can help guide policies to control and eliminate illegal fisheries by implementing self-enforcement and including local communities in small-scale management actions, as has been previously successful in the Raja Ampat Shark and Ray Sanctuary in Indonesia (Stewart et al. 2016). These efforts will help prevent declines in populations of Endangered species such as the giant manta ray in Ecuadorian waters.

LITERATURE CITED

Acuña-Marrero D, Smith ANH, Hammerschlag N, Hearn A and others (2017) Residency and movement patterns of an apex predatory shark (*Galeocerdo cuvier*) at the Galapagos Marine Reserve. PLOS ONE 12:e0183669

Adamack AT, Gruber B (2014) POPGENREPORT: simplifying basic population genetic analyses in R. Methods Ecol Evol 5:384–387

Alcala N, Goudet J, Vuilleumier S (2014) On the transition of genetic differentiation from isolation to panmixia: what we can learn from G_{ST} and *D*. Theor Popul Biol 93:75–84

Allendorf FW, Hohenlohe PA, Luikart G (2010) Genomics and the future of conservation genetics. Nat Rev Genet 11:697–709

Anderson RC, Adam MS, Goes JI (2011) From monsoons to mantas: seasonal distribution of *Manta alfredi* in the Maldives. Fish Oceanogr 20:104–113

Andrzejaczek S, Schallert RJ, Forsberg K, Arnoldi NS, Cabanillas-Torpoco M, Purizaca W, Block BA (2021) Reverse diel vertical movements of oceanic manta rays off the northern coast of Peru and implications for conservation. Ecol Solut Evid 2:e12051

Armstrong AO, Armstrong AJ, Jaine FRA, Couturier LIE and others (2016) Prey density threshold and tidal influence on reef manta ray foraging at an aggregation site on the Great Barrier Reef. PLOS ONE 11:e0153393

Arthofer W, Heussler C, Krapf P, Schlick-Steiner BC, Steiner FM (2018) Identifying the minimum number of microsatellite loci needed to assess population genetic structure: a case study in fly culturing. Fly (Austin) 12:13–22

Beale CS, Stewart JD, Setyawan E, Sianipar AB, Erdmann MV (2019) Population dynamics of oceanic manta rays (*Mobula birostris*) in the Raja Ampat Archipelago, West Papua, Indonesia, and the impacts of the El Niño–Southern Oscillation on their movement ecology. Divers Distrib 25:1472–1487

Benbouza H, Jacquemin JM, Baudoin JP, Mergeai G (2006) Optimization of a reliable, fast, cheap and sensitive silver staining method to detect SSR markers in polyacrylamide gels. Biotechnol Agron Soc Environ 10:77–81

Bester-van der Merwe AE, Gledhill KS (2015) Molecular species identification and population genetics of chondrichthyans in South Africa: current challenges, priorities and progress. Afr Zool 50:205–217

Blacket MJ, Robin C, Good RT, Lee SF, Miller AD (2012) Universal primers for fluorescent labelling of PCR fragments — an efficient and cost-effective approach to genotyping by fluorescence. Mol Ecol Resour 12:456–463

Bray DJ (2018) Family Mobulidae. https://fishesofaustralia.net.au/Home/family/298 (accessed 11 July 2020)

Broderick D, Ovenden JR, Buckworth RC, Newman SJ, Lester RJG, Welch DJ (2011) Genetic population structure of grey mackerel *Scomberomorus semifasciatus* in northern Australia. J Fish Biol 79:633–661

Burgess K (2017) Feeding ecology and habitat use of the giant manta ray *Manta birostris* at a key aggregation site off mainland Ecuador. PhD thesis, The University of Queensland, Brisbane

Chapuis MP, Estoup A (2007) Microsatellite null alleles and estimation of population differentiation. Mol Biol Evol 24:621–631

Chen B, Cole JW, Ginsbach CG (2017) Departure from Hardy Weinberg equilibrium and genotyping error. Front Genet 8:167

Clark T (2002) Population structure of *Manta birostris* (Chondrichthyes: Mobulidae) from the Pacific and Atlantic oceans. MSc thesis, Texas A&M University, College Station, TX

Couturier LIE, Marshall AD, Jaine FRA, Kashiwagi T and others (2012) Biology, ecology and conservation of the Mobulidae. J Fish Biol 80:1075–1119

Couturier LIE, Jaine FRA, Kashiwagi T (2015) First photographic records of the giant manta ray *Manta birostris* off eastern Australia. PeerJ 3:e742

Danusevicius D, Kavaliauskas D, Fussi B (2016) Optimum sample size for SSR-based estimation of representative allele frequencies and genetic diversity in Scots pine populations. Balt For 22:194–202

Derous S, Austen M, Claus S, Daan N and others (2007) Building on the concept of marine biological valuation with respect to translating it to a practical protocol: viewpoints derived from a joint ENCORA–MARBEF initiative. Oceanologia 49:579–586

Dewar H, Mous P, Domeier M, Muljadi A, Pet J, Whitty J (2008) Movements and site fidelity of the giant manta ray,

Manta birostris, in the Komodo Marine Park, Indonesia. Mar Biol 155:121–133

Domingues RR, Hilsdorf AWS, Gadig OBF (2018) The importance of considering genetic diversity in shark and ray conservation policies. Conserv Genet 19:501–525

Dulvy NK, Pardo SA, Simpfendorfer CA, Carlson JK (2014) Diagnosing the dangerous demography of manta rays using life history theory. PeerJ 2:e400

Earl DA, VonHoldt BM (2012) STRUCTURE HARVESTER: a website and program for visualizing STRUCTURE output and implementing the Evanno method. Conserv Genet Resour 4:359–361

Echevin V, Colas F, Chaigneau A, Penven P (2011) Sensitivity of the Northern Humboldt Current System nearshore modeled circulation to initial and boundary conditions. J Geophys Res Oceans 116:C07002

Edgar GJ, Banks SA, Brandt M, Bustamante RH and others (2010) El Niño, grazers and fisheries interact to greatly elevate extinction risk for Galapagos marine species. Glob Change Biol 16:2876–2890

ESRI (Environmental Systems Research Institute) (2020) ArcGIS desktop: release 10. https://desktop.arcgis.com (accessed 30 December 2020)

Evanno G, Regnaut S, Goudet J (2005) Detecting the number of clusters of individuals using the software STRUCTURE: a simulation study. Mol Ecol 14:2611–2620

Excoffier L, Lischer HEL (2010) Arlequin suite ver 3.5: a new series of programs to perform population genetics analyses under Linux and Windows. Mol Ecol Resour 10:564–567

Farmer NA, Garrison LP, Horn C, Miller M and others (2022) The distribution of manta rays in the western North Atlantic Ocean off the eastern United States. Sci Rep 12: 6544

Fischer MC, Rellstab C, Leuzinger M, Roumet M and others (2017) Estimating genomic diversity and population differentiation — an empirical comparison of microsatellite and SNP variation in *Arabidopsis halleri*. BMC Genomics 18:69

Grados C, Chaigneau A, Echevin V, Dominguez N (2018) Upper ocean hydrology of the Northern Humboldt Current System at seasonal, interannual and interdecadal scales. Prog Oceanogr 165:123–144

Graham RT, Witt MJ, Castellanos DW, Remolina F, Maxwell S, Godley BJ, Hawkes LA (2012) Satellite tracking of manta rays highlights challenges to their conservation. PLOS ONE 7:e36834

Hearn AR, Acuña D, Ketchum JT, Peñaherrera C and others (2014) Elasmobranchs of the Galapagos Marine Reserve. In: Denkinger J, Vinueza L (eds) The Galapagos marine reserve: a dynamic social–ecological system. Springer, Cham, p 23–59

Hook SA (2017) The application of genetics and proteomics for the conservation of sharks and their relatives. PhD thesis, The University of Manchester

Hosegood J (2020) Genomic tools for conservation and management of manta and devil rays (*Mobula* Spp.). PhD thesis, Bangor University

IMARPE (Instituto del Mar del Perú) (2021) Índice Costero El Niño (ICEN). www.imarpe.gob.pe/imarpe/index2.php?id_seccion=I0178090300000000000000 (accessed 4 June 2021)

IUCN (2020) The IUCN Red List of Threatened Species. https://www.iucnredlist.org/species/198921/214397182 (accessed 21 December 2020)

Jakobsson M, Rosenberg NA (2007) CLUMPP: a cluster matching and permutation program for dealing with label switching and multimodality in analysis of population structure. Bioinformatics 23:1801–1806

Jombart T (2008) adegenet: a R package for the multivariate analysis of genetic markers. Bioinformatics 24:1403–1405

Kamvar ZN, Tabima JF, Grünwald NJ (2014) Poppr: an R package for genetic analysis of populations with clonal, partially clonal, and/or sexual reproduction. PeerJ 2:e281

Kashiwagi T, Marshall AD, Bennett MB, Ovenden JR (2011) Habitat segregation and mosaic sympatry of the two species of manta ray in the Indian and Pacific Oceans: *Manta alfredi* and *M. birostris.* Mar Biodivers Rec 4:e53

Kashiwagi T, Broderick D, Lance SL, Bennett MB, Ovenden JR (2012) Development and characterization of ten microsatellite loci for the reef manta ray *Manta alfredi.* Conserv Genet Resour 4:1055–1058

Kashiwagi T, Maxwell EA, Marshall AD, Christensen AB (2015) Evaluating manta ray mucus as an alternative DNA source for population genetics study: underwater-sampling, dry-storage and PCR success. PeerJ 3:e1188

Keenan K, McGinnity P, Cross TF, Crozier WW, Prodöhl PA (2013) diveRsity: an R package for the estimation and exploration of population genetics parameters and their associated errors. Methods Ecol Evol 4:782–788

Lassauce H, Dudgeon CL, Armstrong AJ, Wantiez L, Carroll EL (2022) Evidence of fine-scale genetic structure for reef manta rays *Mobula alfredi* in New Caledonia. Endang Species Res 47:249–264

Lezama-Ochoa N, Hall M, Román M, Vogel N (2019a) Spatial and temporal distribution of mobulid ray species in the eastern Pacific Ocean ascertained from observer data from the tropical tuna purse-seine fishery. Environ Biol Fishes 102:1–17

Lezama-Ochoa N, Hall MA, Pennino MG, Stewart JD, López J, Murua H (2019b) Environmental characteristics associated with the presence of the spinetail devil ray (*Mobula mobular*) in the eastern tropical Pacific. PLOS ONE 14:e0220854

Lieber L, Hall G, Hall J, Berrow S and others (2020) Spatio-temporal genetic tagging of a cosmopolitan planktivorous shark provides insight to gene flow, temporal variation and site-specific re-encounters. Sci Rep 10:1661

Lowe WH, Allendorf FW (2010) What can genetics tell us about population connectivity? Mol Ecol 19:3038–3051

Marandel F, Lorance P, Andrello M, Charrier G, LeCam S, Lehuta S, Trenkel VM (2018) Insights from genetic and demographic connectivity for the management of rays and skates. Can J Fish Aquat Sci 75:1291–1302

Marshall A (2008) Biology and population ecology of *Manta birostris* in southern Mozambique. PhD thesis, The University of Queensland, Brisbane

Marshall A, Compagno L, Bennett M (2009) Redescription of the genus *Manta* with resurrection of *Manta alfredi* (Krefft, 1868) (Chondrichthyes; Myliobatoidei; Mobulidae). Zootaxa 2301:1–28

Marshall A, Bennett MB, Kodja G, Hinojosa-Alvarez S and others (2011a) *Manta birostris.* The IUCN Red List of Threatened Species 2011: e.T198921A9108067

Marshall AD, Dudgeon CL, Bennett MB (2011b) Size and structure of a photographically identified population of manta rays *Manta alfredi* in southern Mozambique. Mar Biol 158:1111–1124

McClain CR, Balk MA, Benfield MC, Branch TA and others (2015) Sizing ocean giants: patterns of intraspecific size variation in marine megafauna. PeerJ 3:e715

Milton DA, Shaklee JB (1987) Biochemical genetics and population structure of blue grenadier, *Macruronus novaezelandiae* (Hector) (Pisces: Merluccidae), from Australian waters. Mar Freshw Res 38:727–742

Montecino V, Lange CB (2009) The Humboldt Current System: ecosystem components and processes, fisheries, and sediment studies. Prog Oceanogr 83:65–79

Moreno B, Gonzalez-Pestana A (2017) Southernmost record of the giant manta ray *Mobula birostris* (Walbaum, 1792) in the Eastern Pacific. Mar Biodivers Rec 10:27

O'Malley MP, Lee-Brooks K, Medd HB (2013) The global economic impact of manta ray watching tourism. PLOS ONE 8:e65051

Osgood GJ, White ER, Baum JK (2021) Effects of climate-change-driven gradual and acute temperature changes on shark and ray species. J Anim Ecol 90:2547–2559

Palomino A, Guerrero M, Hearn A (2020) Informe final sobre monitoreo de megafauna marina (*Mobula birostris* y *Rhincodon typus*) usando métodos satelitales y acústicos para entender los patrones de distribución poblacional y movimientos migratorios para optimizar las medidas de conservación. Proyecto IKU, Fundación Megafauna Marina del Ecuador & World Wide Fund, Ecuador

Paradis E, Schliep K (2019) ape 5.0: an environment for modern phylogenetics and evolutionary analyses in R. Bioinformatics 35:526–528

Pardini AT, Jones CS, Scholl MC, Noble LR (2000) Isolation and characterization of dinucleotide microsatellite loci in the great white shark, *Carcharodon carcharias*. Mol Ecol 9:1176–1178

Pew J, Muir PH, Wang J, Frasier TR (2015) related: an R package for analyzing pairwise relatedness from codominant molecular markers. Mol Ecol Resour 15:557–561

Pritchard JK, Stephens M, Donnelly P (2000) Inference of population structure using multilocus genotype data. Genetics 155:945–959

Putman AI, Carbone I (2014) Challenges in analysis and interpretation of microsatellite data for population genetic studies. Ecol Evol 4:4399–4428

Putra MIH, Setyawan E, Laglbauer BJ, Lewis S, Dharmandi D, Sianipar A, Ender I (2020) Predicting mobulid ray distribution in coastal areas of Lesser Sunda Seascape: implication for spatial and fisheries management. Ocean Coast Manage 198:105328

Core Team (2019) R: a language and environment for statistical computing. R Foundation for Statistical Computing, Vienna

Raymond M, Rousset F (1995) GENEPOP (version 1.2): population genetics software for exact tests and ecumenicism. J Hered 86:248–249

Reynolds LK, Stachowicz JJ, Hughes AR, Kamel SJ, Ort BS, Grosberg RK (2017) Temporal stability in patterns of genetic diversity and structure of a marine foundation species (*Zostera marina*). Heredity 118:404–412

Ritland K (2009) Estimators of pairwise relatedness and individual inbreeding coefficients. Genet Res 67: 175–185

Rosenberg NA (2003) distruct: a program for the graphical display of population structure. Mol Ecol Notes 4:137–138

Sandoval-Castillo J (2019) Conservation genetics of elasmobranchs of the Mexican Pacific Coast, trends and perspectives. Adv Mar Biol 83:115–157

Schmidt JV, Schmidt CL, Ozer F, Ernst RE, Feldheim KA, Ashley MV, Levine M (2009) Low genetic differentiation across three major ocean populations of the whale shark, *Rhincodon typus*. PLOS ONE 4:e4988

Seminoff JA, Zárate P, Coyne M, Foley DG, Parker D, Lyon BN, Dutton PH (2008) Post-nesting migrations of Galápagos green turtles *Chelonia mydas* in relation to oceanographic conditions: integrating satellite telemetry with remotely sensed ocean data. Endang Species Res 4:57–72

Sharma R, Kumar B, Arora R, Ahlawat S, Mishra AK, Tantia MS (2016) Genetic diversity estimates point to immediate efforts for conserving the endangered Tibetan sheep of India. Meta Gene 8:14–20

Stewart JD, Beale CS, Fernando D, Sianipar AB, Burton RS, Semmens BX, Aburto-Oropeza O (2016) Spatial ecology and conservation of *Manta birostris* in the Indo-Pacific. Biol Conserv 200:178–183

Stewart JD, Jaine FR, Armstrong AJ, Armstrong AO, Bennett MB, Burgess KB, Stevens GM (2018) Research priorities to support effective manta and devil ray conservation. Front Mar Sci 5:314

Sundqvist L, Keenan K, Zackrisson M, Prodhol P, Kleinhans D (2016) Directional genetic differentiation and relative migration. Ecol Evol 6:3461–3475

Torres ML, Gutiérrez B (2018) A preliminary assessment of the genetic diversity and population structure of guava, *Psidium guajava*, in San Cristobal. In: Torres ML, Mena CF (eds) Understanding invasive species in the Galapagos Islands: from the molecular to the landscape. Springer International Publishing, Cham, p 3–17

Vásquez-Carrillo C, Noriega-Hoyos CL, Hernandez-Rivera L, Jáuregui-Romero GA, Sullivan Sealey K (2020) Genetic diversity and demographic connectivity of Atlantic green sea turtles at foraging grounds in northeastern Colombia, Caribbean Sea. Front Mar Sci 7:96

Vergara-Chen C, Rodrigues F, González-Wangüemert M (2015) Population genetics of *Cerastoderma edule* in Ria Formosa (southern Portugal): the challenge of understanding an intraspecific hotspot of genetic diversity. J Mar Biol Assoc UK 95:371–379

Veríssimo A, Sampaio Í, McDowell JR, Alexandrino P and others (2017) World without borders—genetic population structure of a highly migratory marine predator, the blue shark (*Prionace glauca*). Ecol Evol 7:4768–4781

von Schuckmann K, Le Traon PY, Alvarez-Fanjul E, Axell L and others (2016) The Copernicus Marine Environment Monitoring Service ocean state report. J Oper Oceanogr 9(Suppl 2):s235–s320

Wang J (2002) An estimator for pairwise relatedness using molecular markers. Genetics 160:1203–1215

Wang C, Rosenberg NA (2012) MicroDrop: a program for estimating and correcting for allelic dropout in nonreplicated microsatellite genotypes version 1.01. https://rosenberglab.stanford.edu/software/MicroDrop_Manual.pdf

Wickham H (2009) ggplot2: elegant graphics for data analysis. Springer-Verlag, New York, NY

Yun SA, Son HD, Im HT, Kim SC (2020) Genetic diversity and population structure of the endangered orchid *Pelatantheria scolopendrifolia* (Orchidaceae) in Korea. PLOS ONE 15:e0237546